HYDRAULIC STUDY ON LEVEE ARRANGEMENT ON KUROBE ALLUVIAL FAN CONSTRUCTED IN THE EARLY 19TH CENTURY

TADAHARU ISHIKAWA
Tokyo Institute of Technology, Tokyo, Japan, workishikawa0612@yahoo.co.jp

HIROSHI SENOO
Token C. E. E. Consultants Co., Ltd, Tokyo, Japan, senoo-h@tokencon.co.jp

ABSTRACT

Before the middle of 19th century, discontinuous levee system was commonly adopted in Japan to control river inundations. In this study, the construction process and hydraulic function of the discontinuous levees which were gradually developed on the Kurobe Alluvial Fan during the late 17th and early 19th centuries were investigated being based on old map analysis and numerical flow simulations. The distortion of pictorial map drawn in 1875 was corrected from comparison with the modern map of 1910, and the levee layout in the former was determined. The result clarified that the early fragmentary levees were integrated to the large levee system in the early 19th century and that the early levees were placed mainly on the two sections where the river tended to change its course due to the long-term geomorphological movement; one was near the fan top, and the other was around "the geomorphological nodal point" on the middle of slope of the dissected alluvial fan. The results of numerical flow simulation for the levee arrangement in the early 19th century clarified that an exceeding flood was diverted to the old river channels beside the main channel through "simple levee openings" upstream from the geomorphological nodal point and that a part of diverted flow was returned to the main channel through "funnel-shape levee openings" located on the lower river reach. This fact suggests that the civil engineers of those days knew the geomorphological characteristics of the alluvial fan.

Keywords: Discontinuous levee system, early modern age, hydraulic function, numerical flow simulation

1. INTRODUCTION

In early modern age of Japan (from the 17th to the mid-19th centuries), when hard, continuous levees were not built, a variety of discontinuous levee systems were employed to control river flooding. The systems often functioned well to control floods exceeding a channel capacity (e.g., Ishikawa and Akoh, 2019). The technology of levee design in those days could help flood disaster prevention works in the near future, when the exceeding floods will become more frequent due to the global climate change. However, the scope of knowledge and the strategy of levee design at that time was not completely clarified. In this study, the construction process and hydraulic function of the discontinuous levees which were gradually developed on the Kurobe Alluvial Fan during the late 18th and early 19th centuries were investigated being based on old map analysis and numerical flow simulations.

Three old maps were analyzed to determine the old levee locations. The first was a pictorial map drawn in 1785 (Kurobe Construction Office, Ministry of Construction, 1977), in which the major streams and the levees were marked together with the locations of villages. The second was a modern map published in 1910, in which the villages having the same names as shown in the former were plotted. The third was a levee layout surveyed in the late 19th century under the guidance of a Dutch engineer, which is owned by Toyama Prefectural Library now. Based on geometrical correlation among them, the levee positions were plotted on the latest GIS map.

Numerical flow simulations using shallow water model were conducted for three conditions of levee arrangement: no-levee condition, the group of fragmentary levees of 18th century and the final levee system in the 19th century. The topographic condition for all cases was assumed to be the same as the present one due to the lack of old days data. For the numerical flow simulations, the past maximum flood hydrograph observed in 1969 was reduced to two flood hydrographs the return period of which are 10 and 20 years by considering the flood scale for river planning of the old days. Flow fields obtained from the three cases were compared to estimate the hydraulic function of the levee system, and the flood control strategy of those days was discussed.

2. STUDY SITE DESCRIPTION

2.1 Topography of Kurobe Alluvial Fan

The Kurobe Alluvial Fan is a dissected fan formed by the Kurobe River, which flows down a distance of 85 km from the central mountain range of 3,000 meters high to the Japan Sea Coast, carrying a large volume of sediment from the canyon. The Kurobe Alluvial Fan has a radius of 13 km and an average slope of 1/100 (see Figure 1). The sky-blue bands in the figure represent the old river courses, which tend to branch in the middle of the fan as well as near the top of fan.

The contour lines are beautifully concentric, although the coastline was distorted by erosion and sedimentation in the north and the west parts, respectively after the river changed its course form the north to the west in the mid-16th century. The *J*, *M* and *F-planes* with coloured open arrows are the remains of old fans. Short black lines at the both sides of the present river course represent the levee locations measured at the end of the 19th century. It should be noted that the upstream section has a lot of simple levee openings, whereas the downstream has a series of funnel shape levees which open toward upstream. The meaning of this difference will be discussed later.

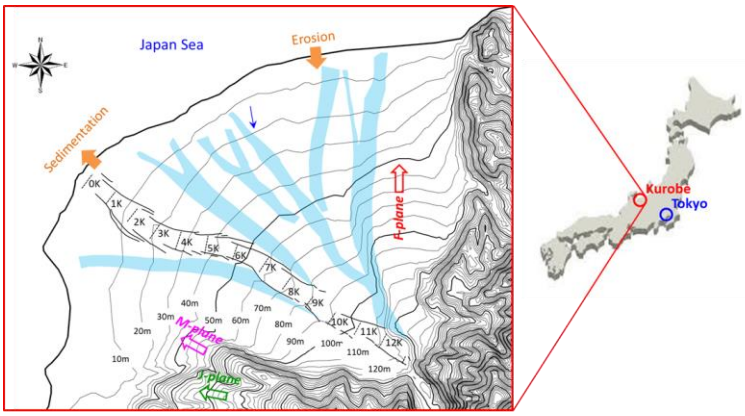

Figure 1. Contour map of the Kurobe Alluvial Fan

2.2 Long-term geomorphological motion

Slope profiles of those fans from the present fan top are plotted in Figure 2, where *P-plane* is the present one, and others are remains of old fans. Carbon-14 dating showed that the fan plane formation was $J \rightarrow M \rightarrow F \rightarrow P$, which coincides with the order of slope degrees. This fact means that the ground of this area has been tilting with time; the mountain side rising, and the seaside sinking. According to various field data, such as the rate of ground rising/sinking, the sea surface change after the Ice Age and the unconformity under the seabed, the variation from *F*-plane to *P*-plane has continued for the last 10,000 years, though those data are not presented here for restriction of space. The lines of *F*- and *P-planes* intersect in the middle of the present fan, which means that erosion occurred on the upper and deposition on the lower half of fan. This geomorphological motion was the cause of the river course changes in the middle of present alluvial fan.

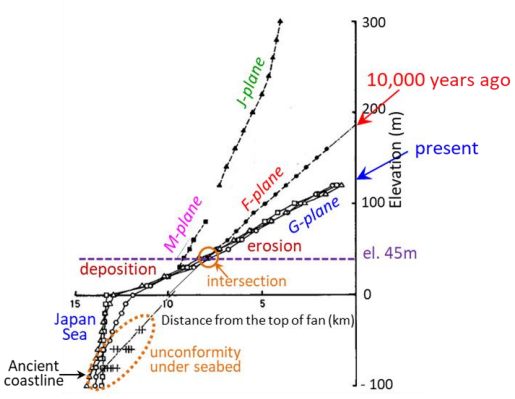

Figure 2. Slope profiles of old and present fans

3. OLD MAP ANALYSIS

Figures 3 shows the old maps which were used in this study. The (a) is the pictorial map drawn in 1785, in which the streams and levees of the Kurobe River were plotted together with village names and main roads. The (b) is a part of the modern map of all over Japan published in 1910, where the location of villages with their names almost common to those in the pictorial map (a) were plotted. The (c) shows the levee arrangements obtained by the measurement in 1894 under the direction of Johannis de Rijke, an engineer from the Netherland (the map is furnished by Toyama Prefectural Library).

First, the levee locations on the map (c) were plotted on the map (b), by comparing the river channel characteristics on the both maps. Next, the distortion of the map (a) was corrected using the Triangular Irregular Network Technique by comparing the locations of the villages, roads and large embankments to those on the map (b). The obtained levees were plotted on the GIS map (2015) for numerical flow simulations which will be described in the section 4. The results are shown in Figures 4.

(a) Pictorial map drawn in 1785 (b) Map published in 1910 (c) Levee survey in 1894

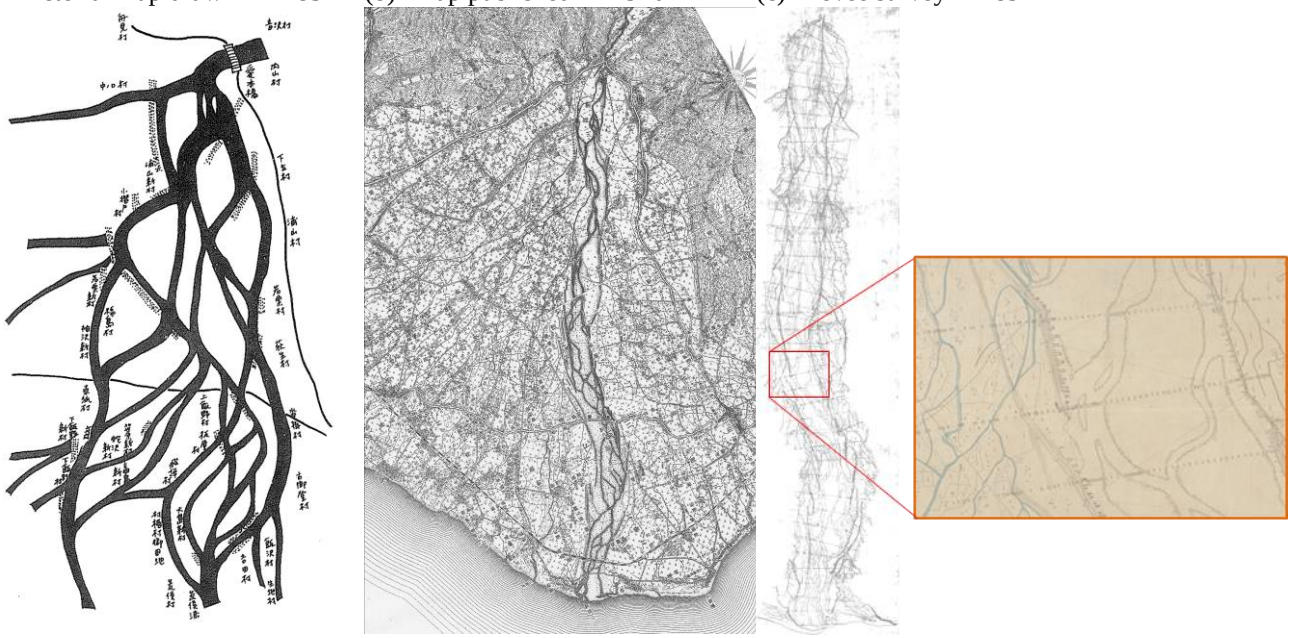

Figure 3. Old maps used in this study

(a) From pictorial map in 1785 (b) From levee survey in 1894

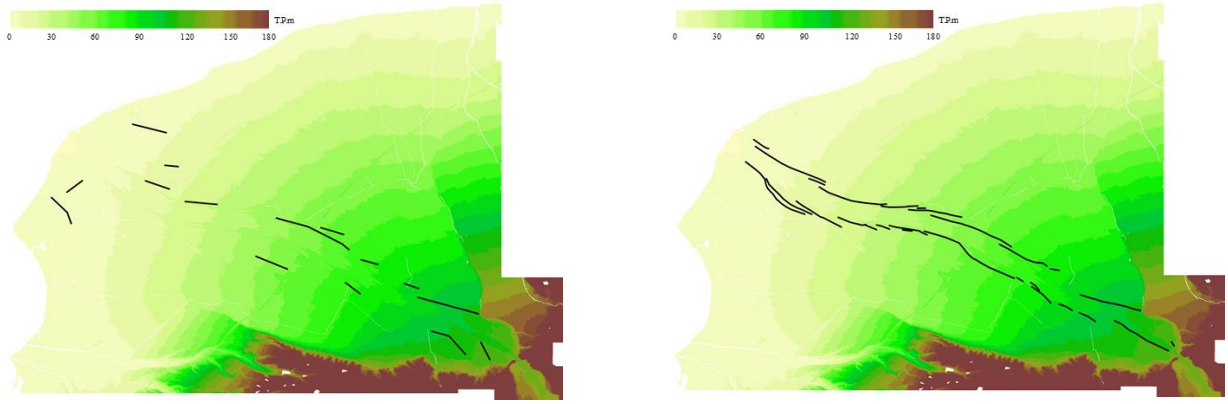

Figure 4. Placement of old levees on the GIS map (2015)

4. NUMERICAL FLOW SIMULATION

4.1 Numerical Simulation Model

A set of shallow water equations was adopted for the numerical simulation model.

$$\frac{\partial h}{\partial t}+\frac{\partial (Uh)}{\partial x}+\frac{\partial (Vh)}{\partial y}=0 \tag{1}$$

$$\frac{\partial (Uh)}{\partial t}+\frac{\partial (UUh)}{\partial x}+\frac{\partial (UVh)}{\partial y} = -gh\frac{\partial H}{\partial x}+\frac{\partial (h\tau_{UU})}{\partial x}+\frac{\partial (h\tau_{UV})}{\partial y}-\frac{\tau_0}{\rho}\frac{U}{\sqrt{U^2+V^2}} \tag{2}$$

$$\frac{\partial (Vh)}{\partial t}+\frac{\partial (UVh)}{\partial x}+\frac{\partial (VVh)}{\partial y} = -gh\frac{\partial H}{\partial y}+\frac{\partial (h\tau_{UV})}{\partial x}+\frac{\partial (h\tau_{VV})}{\partial y}-\frac{\tau_0}{\rho}\frac{V}{\sqrt{U^2+V^2}} \tag{3}$$

where (U, V) are the velocity components in (x, y) coordinates, h is the water depth, H is the water surface level (= h + ground level), ρ is the water density, and g is the gravitational acceleration. τ_0 is the bed friction force, and τ_{UU}, τ_{UV} and τ_{VV} are the horizontal shear stresses, which are expressed by the following equations:

$$\tau_0 = \rho U_f^2 = n^2 \frac{\rho g (U^2 + V^2)}{h^{1/3}}$$
$$\tau_{UU} = 2\varepsilon \frac{\partial U}{\partial x} - \frac{2}{3}k \quad \tau_{UV} = \varepsilon \frac{\partial U}{\partial y} + \varepsilon \frac{\partial V}{\partial x} \quad \tau_{VV} = 2\varepsilon \frac{\partial V}{\partial y} - \frac{2}{3}k \tag{4}$$
$$\varepsilon = \frac{1}{6}\kappa U_f h \qquad k = 2.07 U_f^2$$

where U_f is the friction velocity, n is Manning's roughness coefficient, ε is the vertically averaged eddy viscosity, k is the turbulent kinetic energy, and κ is the Karman constant.

The differential equations were converted to difference equations by the finite volume method on the unstructured triangular mesh system. The equation forms and solving process are described in Akoh et al (2017).

The flow rate over the banks was assumed by the following formula:

$$q = \begin{cases} 0.35 h_1 \sqrt{2 g h_1} & \text{if } h_2 / h_1 \le 2/3 \\ 0.91 h_2 \sqrt{2 g (h_1 - h_2)} & \text{otherwise} \end{cases} \tag{5}$$

where q is the flow rate over the unit length of levee, and h_1 and h_2 are the water depths at the upstream and the downstream sides, respectively, measured from the levee crown.

4.2 Calculation conditions

4.2.1 Topography

Because there have not been any large scale land elevation change after the map-(b) of 1910, the GIS digital elevation data published in 2015 (grid size; 5 m) were basically used for the alluvial fan topography, but some local changes caused by recent constructions of roads and railways were removed by interpolation from surrounding elevation values.

On the other hand, the channel bed elevation was strongly affected by the construction of a high dam in the upstream canyon since1960, and therefore, the digital data were corrected for river bed using the longitudinal profile of laterally averaged channel bed deformation data published by river administration office. In addition, because sandbars of about two-meter high move downstream continuously in the Kurobe River, two topographic data were prepared in order to examine the effect of sandbar pattern on river flooding.

4.2.2 Flood hydrograph

Figure 5(a) shows the design flood hydrograph adopted for the present river improvement works, which was the past maximum flood observed in 1969. This hydrograph was reduced to the peak discharge of 3,000 and 4,000 m^3/s, return periods of which are roughly estimated as 10 and 20 years, according to the probability plot of annual maximum discharge, Figure 5(b). By the way, Flood records in an old document indicated that the villages along the river received flood damages ten times during 68 years from 1828 to 1895, the frequency of flood of which (10/68) corresponds to the discharge of 2,700 m^3/s in Figure 5(b).

(a) Flood hydrograph

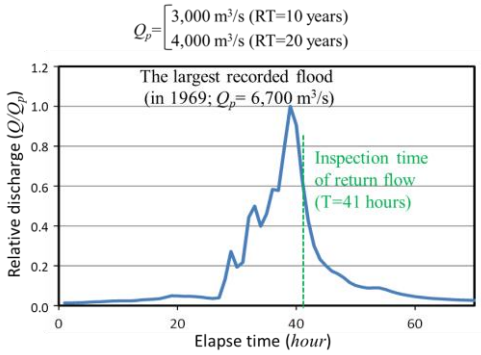

(b) Probability plot of annual maximum discharge

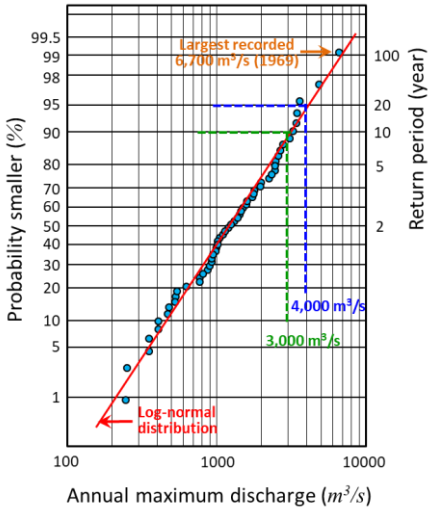

Figure 5. Assumption of floods for numerical simulation.

5. RESULTS AND DISCUSSIONS

5.1 Effect of levee construction in the 18th century

Spatial distributions of water depth h and velocity U were obtained for each calculation time step, and a parameter named hydrodynamic force ($HF=hU^2$) herein was calculated as an index for the flood impact on wooden houses. According to Sato et.al (1989), the HF value was roughly connected to wooden house damage as follows:

HF < 1.5: almost no damage, 1.5 < HF < 2.5: partial damage, 2.5 < HF: total damage.

Figures 6 show the simulation results of HF for Q_p =3,000 and 4,000 m^3/s: The (a) is for no levee condition and the (b) is for levees in 1785. River bed topography was assumed as sandbar pattern-1 which was the original GIS data. The yellow dots with alphabet show the locations of villages. In the cases of no levee condition, many villages at right bank side are inundated, and a few of them are located in the yellow and the red zones. The levees in 1785 reduced the inundation area at the right bank side in the case of Q_p=3,000 m^3/s drastically. Especially, the two long levees cut off the branch flows from the fan top and the middle of slope. However, the effect was not satisfactory in the case of Q_p=4,000 m^3/s. In addition, because there was no long levee at the left bank side, a branch flow from the middle of left bank caused a wide inundation toward four villages near the coast.

(a) no levee condition (Q_p=3,000 m^3/s, *Pattern-1*) (b) levees in 1785 (Q_p=3,000 m^3/s, *Pattern-1*)

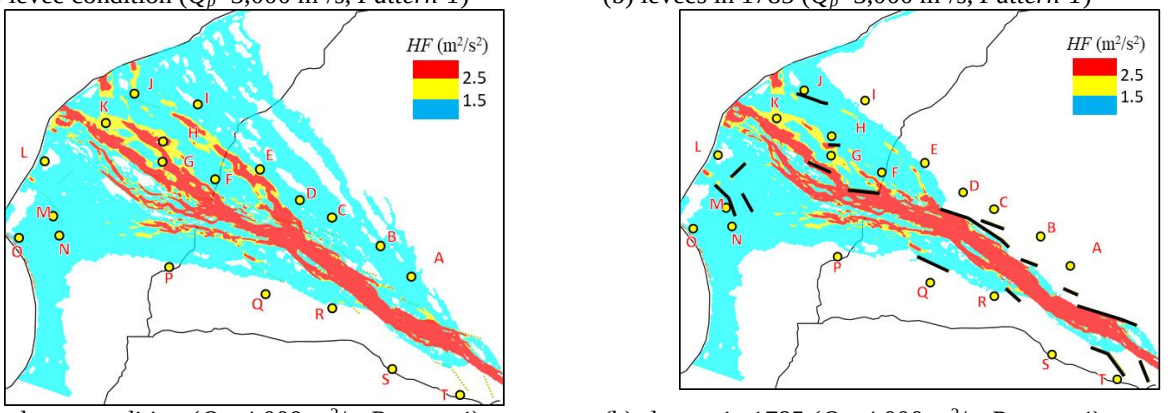

(a) no levee condition (Q_p=4,000 m^3/s, *Pattern-1*) (b) levees in 1785 (Q_p=4,000 m^3/s, *Pattern-1*)

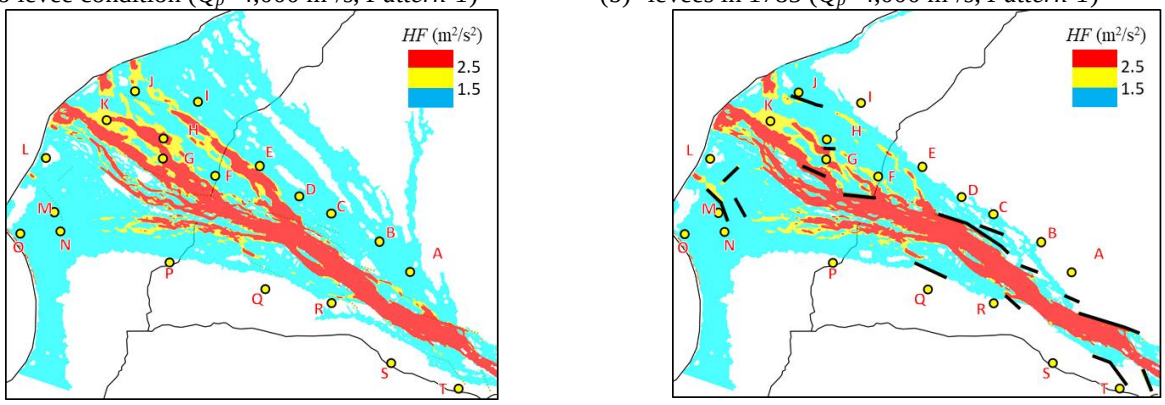

Figures 6: HF distribution showing the effect of levees in 1785

5.2 Hydraulic function of levee system in the mid-19th century

Figures 7 show the HF distributions for the two sandbar patterns as well as the two flood scales, when the levee system was completed. For the sandbar pattern-1, flooding occurred only at the left bank side, but it occurred at the both bank sides for the sandbar pattern-2. This result suggests that the inundation areas changed much depending on the sandbar pattern. Comparison with the corresponding cases shown in Figures 6, it can be clearly found that the completed system of discontinuous levees reduced the flood flow impact on the villages very successfully.

Looking closely, the flooding starts through the simple levee openings of the upstream section, flows through the old river channel beside the main channel which were shown in Figure 1. Figure 8 shows the inundation depth at flood receding phase (the elapse time is 41 hours in Figure 5(a)), together with the velocity vectors in the rectangle areas where the flood flows touches the funnel-shape levees. The flooding water is absorbed into the main channel through the levee openings. These calculation results suggest that the civil engineers in early modern age ingeniously made use of the old river channels as temporary floodways by designing the levee openings.

(a) Q_p=3,000 m^3/s, *Pattern-1*

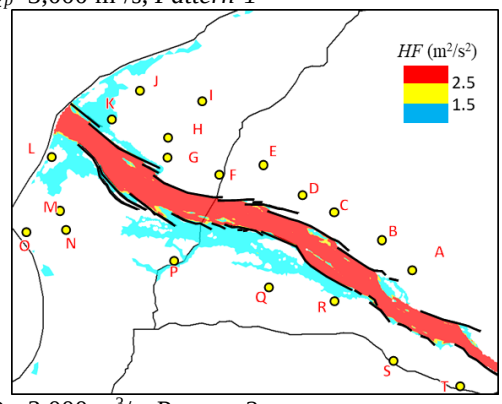

(b) Q_p=4,000 m^3/s, *Pattern-1*

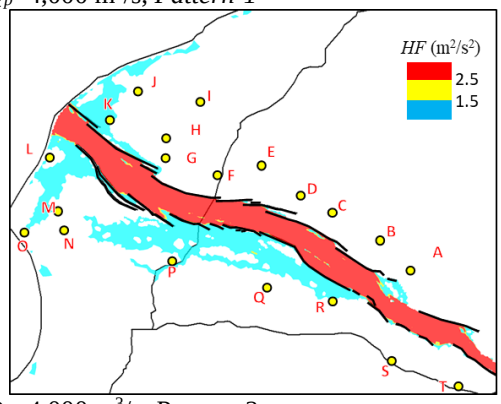

(c) Q_p=3,000 m^3/s, *Pattern-2*

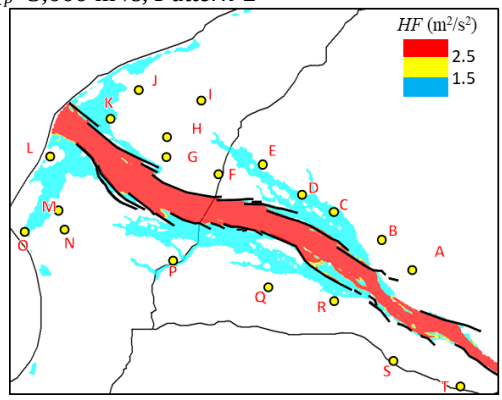

(d) Q_p=4,000 m^3/s, *Pattern-2*

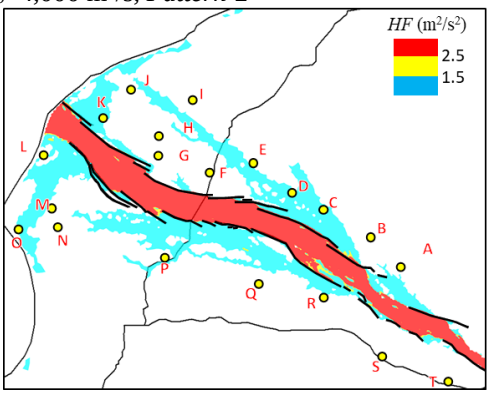

Figure 7. *HF* distribution for the completed levee system in the mid-19th century.

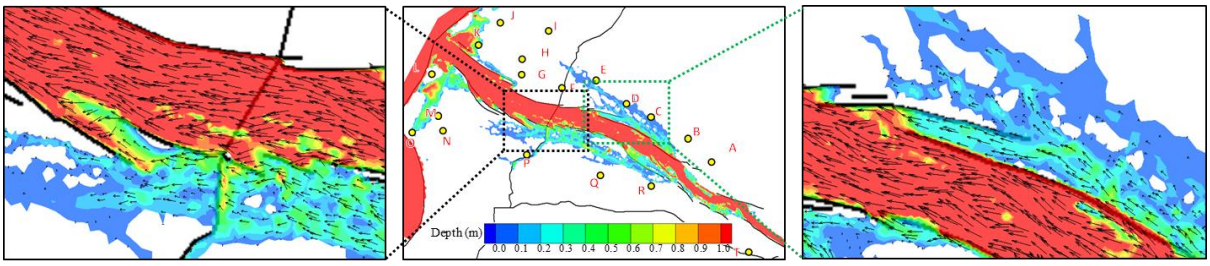

Figure 8. Flood absorption by funnel-shape levee openings

6. CONCLUSIONS

The numerical simulations described above suggested about the design points and hydraulic effects of river levees on the Kurobe Alluvial Fan in early modern age as follows:

1. In the levee construction shown in the pictorial map of 1785, the comparatively long levees were built to cut off the major river branches at the right bank, and other short levees were built to guard individual village from the inundation.
2. Comparison of the two levee arrangements of the late 18th and the mid-19th centuries shows that the former ones were integrated to complete the levee system of latter, although it is not certain if the river engineers in the 18th century already had a blueprint for the latter.
3. In the mid-19th century, old river channels beside the main channel were ingeniously used as temporary floodways when the river discharge exceeded the main channel capacity by adopting two types levee openings; the simple openings for flow divergence in the upstream and the funnel-shape openings in the downstream for returning the inundation water to the main channel after the flood peak.

REFERENCES

Akoh, R., Ishikawa, T., Kojima, T., Tomaru, M. and Maeno, S. (2017). High-resolution modeling of tsunami run-up flooding: a case study of flooding in Kamaishi city, Japan, induced by the 2011 Tohoku tsunami, Nat. Hazards Earth Syst. Sci., 17:1871-1883.

Ishikawa, T. and Akoh, R. (2019). Assessment of flood risk management in lowland Tokyo arears in the seventeenth century by numerical flow simulation, Environmental Fluid Mechanics, 19: 1295-1307.

Kurobe Construction Office, Ministry of Construction (1977). History of the Kurobe River. (in Japanese)

Sato, S, Imamura, F and Shuto, N. (1989). Numerical Simulation of Flood and Damage to Houses-A Case of the Yoshida River due to Typhoon No,8610, Proc. of the Japanese Conference on Hydraulics, 33: 331-336. (in Japanese)